

Article

Impacts of Different Land Use Scenarios on Future Global and Regional Climate Extremes

Tao Hong ¹, Junjie Wu ^{1,2,*}, Xianbiao Kang ¹, Min Yuan ¹ and Lian Duan ¹

¹ College of Aviation Meteorology, Civil Aviation Flight University of China, Guanghan 618307, China; ht@cafuc.edu.cn (T.H.); ht@mail.bnu.edu.cn (X.K.); yuanm@cafuc.edu.cn (M.Y.); dl@cafuc.edu.cn (L.D.)

² Key Laboratory of Flight Techniques and Flight Safety, Civil Aviation Administration of China, Guanghan 618307, China

* Correspondence: wjj@cafuc.edu.cn; Tel.: +86-18981026947

Abstract: Land use and land cover change (LULCC) alters the character of the land surface and directly impacts the climate. The impacts of LULCC on historical and future climate have been largely investigated, mostly using simulations with or without land use change. However, it is still not clear to what extent the projections of future climate change depend on the choice of land use scenario, which can provide important guidance on using land use and land management as a tool for regional climate mitigation. Here, using ten Earth system models participating in future land use policy sensitivity experiments in Land Use Model Intercomparison Project (LUMIP), we assessed the impact of two different land use scenarios (SSP1-2.6 and SSP3-7.0) on extreme climate. The results demonstrate that the use of different land use change scenarios has a substantial effect on the projections of regional climate extreme changes. Our study also reveals that, compared with other anthropogenic forcings, land use change has a considerable contribution to regional temperature extreme changes, with the contribution ranging from -14.0% to 10.3% , and the contribution to regional precipitation extreme change is larger, with a range of -118.4% – 138.8% . The global climate effects of land use change are smaller in magnitude than regional effects, with a small (5%) contribution to temperature extreme change. We also found a large spread in the model's responses to LULCC, especially for precipitation extremes, suggesting that observation-based studies on reducing models' uncertainties are needed to obtain more robust future projections of regional climate change. Our study highlights the essential role of land use and land management strategies in future regional climate mitigation.

Keywords: land use scenario; extreme climate; LUMIP; CMIP6



Citation: Hong, T.; Wu, J.; Kang, X.; Yuan, M.; Duan, L. Impacts of Different Land Use Scenarios on Future Global and Regional Climate Extremes. *Atmosphere* **2022**, *13*, 995. <https://doi.org/10.3390/atmos13060995>

Academic Editor: Carlos E. Ramos Scharrón

Received: 24 May 2022

Accepted: 18 June 2022

Published: 20 June 2022

Publisher's Note: MDPI stays neutral with regard to jurisdictional claims in published maps and institutional affiliations.



Copyright: © 2022 by the authors. Licensee MDPI, Basel, Switzerland. This article is an open access article distributed under the terms and conditions of the Creative Commons Attribution (CC BY) license (<https://creativecommons.org/licenses/by/4.0/>).

1. Introduction

Human activities have modified the environment and climate for many years. Land use and land cover change (LULCC) is one of the major anthropogenic drivers of human-caused climate change. LULCC is a process by which human activities transform the natural landscape, primarily through deforestation, urbanization and the conversion of natural vegetation with cropland and pastures. LULCC influences the climate from local and regional to global scales by changing the land surface characteristics and altering the physical and biogeochemical properties of the terrestrial surfaces [1]. Land management, such as irrigation, the use of fertilizers and pesticides and wood harvesting, can contribute to reducing the negative impacts of climate change.

Anthropogenic LULCC has significant impacts on the Earth's climate, carbon cycle and water balance. Typically, LULCC alters the biophysical properties of the land cover, such as albedo, evapotranspiration and roughness, which in turn affects land–atmosphere energy and water exchange [2]. LULCC can also affect the carbon cycle between the land and atmosphere through biogeochemical emissions and uptake [3]. Historical LULCC has been found to have significant impacts on climate; for example, model-based studies have

shown that historical deforestation in boreal regions may increase surface albedo and lead to local cooling, and deforestation in tropical regions may decrease evapotranspiration and lead to local warming [4,5]. However, there are still large uncertainties in the sign and magnitude of the models' responses [1,6]. Observational studies show that the climate effects of historical deforestation are latitude-dependent [7,8].

Although the radiative forcing of LULCC is far less than that of greenhouse gases, LULCC has an impact of similar or even larger magnitude than greenhouse gases at local to regional scales [9,10]. Studies have emphasized that LULCC should be taken into account in projections of future climate change [11,12]. Future land use change can modify atmospheric heat flux, moisture flux and radiation flux, and have a substantial impact on regional atmospheric variables (temperature, precipitation, cloud, wind, etc.) and hydrological variables (evaporation, soil moisture) [5]. Using CMIP5 models, Brovkin et al. [13] revealed that, in the global mean, the effects of the RCP8.5 land use scenario on climate are significant for regions with land use change exceeding 10%.

LULCC can also affect extremes. LULCC changes energy fluxes and their partitioning and this can amplify or suppress meteorologically driven extremes [1,2]. Model-based results have shown that the impact of LULCC on heat extremes is greater than that of mean temperature. For instance, using four climate models, Pitman et al. [14] found that the impact of historical LULCC on temperature extremes is significant in regions with intense land cover modification, and the magnitude of the LULCC-induced changes can be of similar magnitude to that of CO₂-induced changes. Using observation-constrained climate models, Lejeune et al. [15] found that deforestation increased the intensity of hot days over northern mid-latitudes. However, inconsistent results remain in the models' responses of temperature extremes to LULCC, especially in mid-latitudes. Several models showed that deforestation in mid-latitudes was accompanied by an increase in the occurrence of hot dry summers [16–18], while other models simulated a decrease in warm extreme temperatures [10,19]. In addition, observational studies show that historical LULCC, such as cropland intensification and irrigation, has a substantial impact on regional temperature extremes [20,21].

The role of LULCC in affecting temperature extremes has been compared with that of other anthropogenic forcings. For example, Niu et al. [22] shows that future LULCC-related changes in temperature extremes can be as large as 25% of CO₂-induced changes. Hirsch et al. [23] shows that the responses of temperature extremes to future land use change in low-emission scenarios are comparable in magnitude to those arising from half a degree of global warming. Sy et al. [24] investigated the impact of common future land use scenarios (RCP8.5 and RCP2.6) on climate extremes and found that LULCC substantially modulated projected weather extremes. In addition, the role of LULCC in affecting rainfall is less clear and the responses to future LULCC changes in precipitation extremes are shown to be less statistically significant [14,25].

Previous model-based studies of LULCC's impacts mostly used idealized land use change scenarios, typically such as simulations with and without LULCC under historical climate conditions or future climate change scenarios [26,27], or simulations with idealized extreme land cover changes [28,29]. However, it is still not clear to what extent the projection of future climate change depends on the choice of land use scenario. The choice of land use scenario in low-emission scenarios was shown to largely determine whether the climate projections that limit global warming to well below 1.5 can be achieved [23]. Moreover, different land use scenarios were projected according to levels of human demand for agriculture in the SSP [30]. It is thus worth further exploring the impact of the use of different land use scenarios on the future climate, especially on the regional extreme climate, and assessing whether land use and land management can help to mitigate regional climate change. In addition, most previous studies are often limited to a single or fewer models, or to a few extreme climate indices [12,16,19], which cannot provide sufficient samples to assess the uncertainties of models' responses.

In this study, using simulations from ten Earth system models (ESMs) with two land use scenarios (i.e., SSP1-2.6 and SSP3-7.0, which diverge strongly in land use trends), we compare the responses of climate extremes to these two land use scenarios under different CO₂ concentrations and radiation forcing levels, and assess whether land use and land management can contribute to regional climate mitigation. Furthermore, we also assess the relative contribution of the use of different land use scenarios to global and regional climate extreme change.

2. Methods

2.1. Models and Experiments

The Land Use Model Intercomparison Project (LUMIP) [31] is part of the CMIP6 (Coupled Model Intercomparison Project Phase 6), which aims to further advance our understanding of the impacts of LULCC on climate. This study uses outputs from the future land use policy sensitivity experiments of Phase 2 of LUMIP.

Derivatives from ScenarioMIP (Scenario Model Intercomparison Project) [32], ssp126 (simulation following RCP2.6 global forcing pathway with SSP1 socioeconomic conditions) and ssp370 (simulation following RCP7.0 global forcing pathway with SSP3 socioeconomic conditions), are used as baseline simulations. For each baseline simulation, two sets of simulations are conducted. For example, for the ssp126 baseline simulation, the first set includes the ssp126 simulation from CMIP6 runs with all anthropogenic forcings including the SSP1-2.6 land use scenario; the second set includes the ssp126-ssp370Lu (“SSP1-2.6 with SSP3-7.0 land use”) simulation, all forcings of which are identical to ssp126, except that the land use scenario is taken from ssp370. Similarly, for the ssp370 baseline simulation, the first set includes the ssp370 simulation with the SSP3-7.0 land use scenario; the second set includes the ssp370-ssp126Lu (“SSP3-7.0 with SSP1-2.6 land use”) simulation, which is identical to ssp370, except that the SSP1-2.6 land use scenario is used. Therefore, the difference between the ssp126-370Lu (ssp370-ssp126Lu) and ssp126 (ssp370) simulations corresponds to the influence of land use change. These experiments can be used to assess whether land use and land management strategies can help to mitigate future climate change. All simulations analyzed in this study are summarized in Table 1.

Table 1. Summary of CMIP6 experiments used in this study.

Experiment	Experiment Forcings	Experiment Description	Years
historical	Historical with all forcings	CMIP6 historical simulation	1850–2014
ssp126	Projection with SSP1-2.6 scenario	CMIP6 low forcing scenario projection based on SSP1-2.6	2015–2100
ssp126-ssp370Lu	SSP1-2.6 with SSP3-7.0 land use	Same as ssp126 except for use of SSP3-7.0 land use scenario	2015–2100
ssp370	Projection with SSP3-7.0 scenario	CMIP6 high forcing scenario projection based on SSP3-7.0	2015–2100
ssp370-ssp126Lu	SSP3-7.0 with SSP1-2.6 land use	Same as ssp370 except for use of SSP1-2.6 land use scenario	2015–2100

These particular sets of simulations are used because land use in SSP1-2.6 and SSP3-7.0 diverges strongly. The SSP1-2.6 land use scenario represents a strongly regulated land use future, which includes strongly reduced tropical deforestation and massive reforestation, leading to a significant increase in forest area and little expansion of cropland and pasture areas (Supplementary Materials Figure S1). In contrast, SSP3-7.0 considers a world where land use change is hardly regulated, with the highest increase in cropland and pasture and a large reduction in forest area (Supplementary Materials Figure S1). Other land use scenarios, such as SSP5-8.5, SSP2-4.5 and SSP4-6.0, have moderate land use futures, in which the changes in agricultural land and forest cover are between those in the SSP1-2.6

and SSP3-7.0 land use scenarios [30,31]. Thus, the two land use scenarios used in the simulations represent a broad range of potential land use futures.

This study uses outputs of daily precipitation, surface air temperature, maximum and minimum air temperature from 10 CMIP6 models (ACCESS-ESM1-5, BCC-CSM2-MR, CanESM5, CESM2, CMCC-ESM2, CNRM-ESM2-1, IPSL-CM6A-LR, MPI-ESM1-2-LR, NorESM2-LM, UKESM1-0-LL) participating in LUMIP, the model in which daily outputs from 2015 to 2099 of all four simulations (ssp126, ssp126-ssp370lu, ssp370, ssp370-ssp126lu) are all available is selected, and all available realizations of the model are used. For CESM2, the outputs of daily maximum and minimum temperature of the four simulations are not available. All models' outputs are interpolated to a common 2-degree grid. The details of that models used are listed in Table 2.

Table 2. A brief description of CMIP6 models used in this study.

Model	Horizontal Resolution (Lat × Lon)	Dynamic Vegetation	Number of Plant Functional Types (PFT)	References
ACCESS-ESM1-5	1.2° × 1.9°	No	9	[33]
BCC-CSM2-MR	1.1° × 1.1°	No	15	[34]
CanESM5	2.8° × 2.8°	Yes	9	[35]
CESM2	1.0° × 1.0°	Yes	15	[36]
CMCC-ESM2	0.9° × 1.25°	Yes	16	[37]
CNRM-ESM2-1	1.4° × 1.4°	Yes	9	[38]
IPSL-CM6A-LR	1.9° × 3.8°	No	15	[39]
MPI-ESM1-2-LR	1.9° × 1.9°	Yes	12	[40]
NorESM2-LM	1.9° × 2.5°	No	15	[41]
UKESM1-0-LL	1.3° × 1.9°	Yes	13	[42]

2.2. Climate Extreme Indices

We selected 20 climate extreme indices from the CCI/WCRP/JCOMM Expert Team on Climate Change Detection and Indices (ETCCDI). The definition and the calculation of these climate indices can be found at Climdex (<https://www.climdex.org/learn/indices/>, last access: 23 May 2022), and the selected extreme indices are described in Supplementary Materials Table S1. We used iclim (Index Calculation for CLIMate), which is a Python library to calculate climate indices, based on daily precipitation, daily maximum and minimum air temperature (see <https://iclim.readthedocs.io/en/latest/index.html>, last access: 23 May 2022).

To access the relative contribution of land use change to future regional climate change, the influences of land use change and other anthropogenic forcings are compared, and the relative contribution of land use change is calculated as

$$\text{LULCC}_{126} \text{ effect} = \left| \frac{\text{ssp126_ssp370Lu} - \text{ssp126}}{\text{ssp126} - \text{historical}} \right| \quad (1)$$

$$\text{LULCC}_{370} \text{ effect} = \left| \frac{\text{ssp370_ssp126Lu} - \text{ssp370}}{\text{ssp370} - \text{historical}} \right| \quad (2)$$

where *ssp126*, *ssp126-ssp370Lu*, *ssp370* and *ssp370-ssp126Lu* correspond to global or regional averaged extreme indices over 2076–2100, and *historical* corresponds to the global or regional averaged extreme indices over 1991–2015; therefore, (1) and (2) can be interpreted as the contribution of land use change to total future climate change. In addition, to examine regional changes, we selected 26 regions (Supplementary Materials Figure S4) defined by IPCC AR5 Reference Regions (See https://www.ipcc-data.org/guidelines/pages/ar5_regions.html, last access: 23 May 2022).

3. Results

3.1. Spatial Pattern of the Impact of Different Land Use Scenarios on Extreme Indices

Figure 1 shows the multi-model ensemble spatial distribution of the impact of land use change ($\text{ssp126}-\text{ssp370Lu}-\text{ssp126}$) under the SSP1-2.6 scenario. For mean temperature, using the SSP3-7.0 land use scenario generally leads to cooling in the boreal middle and high latitudes, and warming in tropical Africa (Figure 1a), which is associated with the change in forest cover in these regions. Compared with the SSP1-2.6 land use scenario, the SSP3-7.0 land use scenario mainly increases the forest cover in East Asia and Western Europe and reduces the forest cover in tropical Africa and South America in most models (Supplementary Materials Figures S2 and S3).

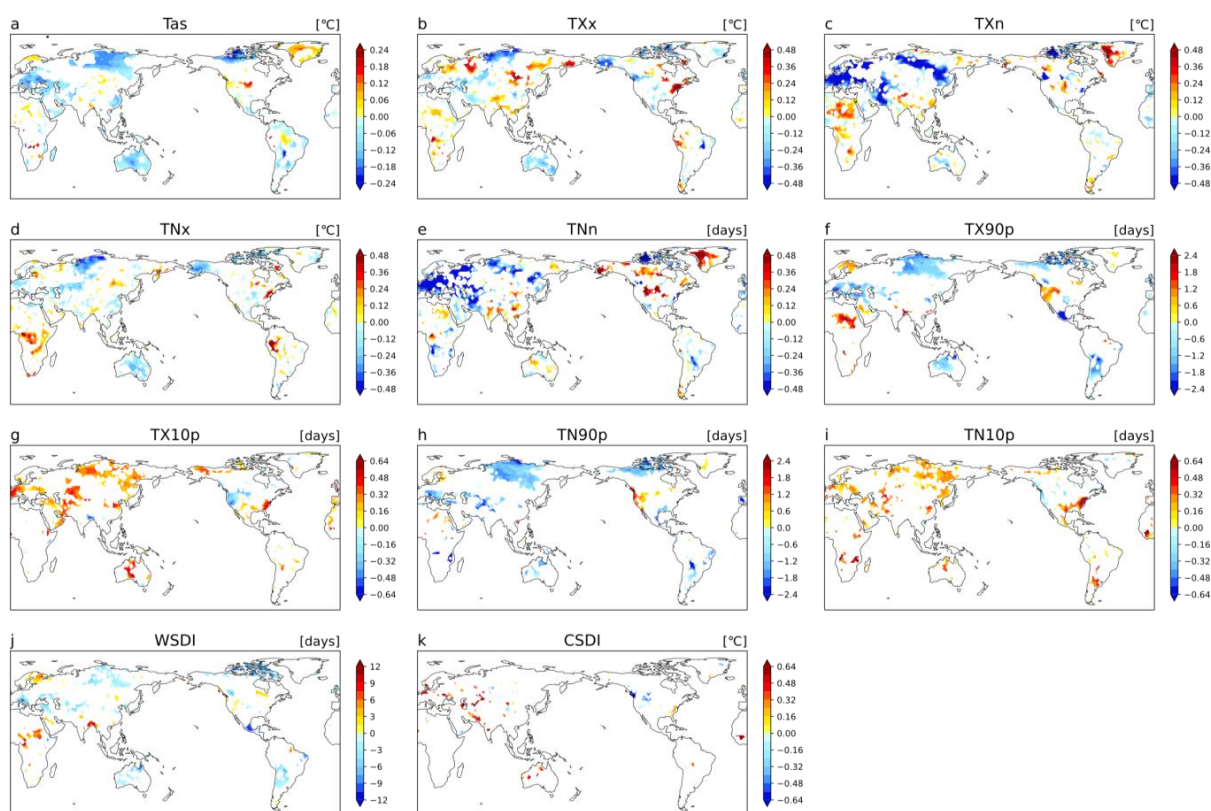


Figure 1. Under SSP1-2.6 scenario, the multi-model ensemble spatial patterns of the impact of land use change (i.e., $\text{ssp126}-\text{ssp370Lu}-\text{ssp126}$) on future temperature extremes. Extreme climate indices are averaged over 2070–2099. Only grid points where at least 70% of the selected CMIP6 models simulate the same anomaly sign are shown. (a) mean temperature, (b) TXx, (c) TXn, (d) TNx, (e) TNn, (f) TX90p, (g) TX10p, (h) TN90p, (i) TN10p, (j) WSDI, (k) CSDI.

For the temperature intensity extremes (TXx, TXn, TNx, TNn), under the SSP1-2.6 scenario, the use of the SSP3-7.0 land use scenario ($\text{ssp126}-\text{ssp370Lu}-\text{ssp126}$) has a significant impact on these indices in most parts of the global land areas (Figure 1b–e), and the magnitude of these temperature extreme changes is larger and almost twice that of the mean temperature changes. The spatial patterns of these temperature intensity extreme responses to the land use change ($\text{ssp126}-\text{ssp370Lu}-\text{ssp126}$) are broadly similar. TXx, TXn, TNx and TNn have increased significantly in tropical Africa and decreased in the boreal high latitudes, which is associated with the forest cover changes in these regions in the SSP3-7.0 land use scenario (Supplementary Materials Figure S2). Furthermore, the magnitude of the cold extreme (TXn and TNn) changes is greater than those of the hot extremes (TXx and TNx).

For the temperature frequency extremes (TX90p, TX10p, TN90p, TN10p), under the SSP1-2.6 scenario, using the SSP3-7.0 land use scenario leads to generally decreased hot

extreme days (TX90p and TN90p) over boreal high latitudes, the Mediterranean, Central Asia, Australia and South America, and increased hot extreme days in tropical Africa and western North America, while changes in cold extreme days (TX10p and TN10p) show almost the opposite spatial patterns (Figure 1f–i). As with the temperature duration extremes (WSDI, CSDI), Figure 1j shows the significantly increased duration of hot extremes (WSDI) over tropical Africa and South Asia, and decreased WSDI over boreal high latitudes. The change in CSDI (duration of cold extremes) is small and not significant over most global land areas (Figure 1k). We also examined the impact of different land use scenarios under the SSP3-7.0 scenario, and found that the replacement of SSP3-7.0 with the SSP1-2.6 land use scenario (i.e., ssp370-ssp126Lu-ssp370) leads to generally similar spatial patterns of temperature extreme changes to those in the SSP1-2.6 baseline simulation (Supplementary Materials Figure S5), except for the strongly increased TXn and TNn over Northeast Asia (Supplementary Materials Figure S5c,e). Overall, the magnitude of temperature extreme changes under the SSP3-7.0 scenario is smaller than that under the SSP1-2.6 scenario.

Figure 2 shows the spatial patterns of the impact of using the SSP3-7.0 land use scenario (ssp126-370Lu-ssp126) on precipitation; the mean precipitation shows decreases over South Asia and South America, and increases over Western Europe (Figure 2a). Precipitation extremes change broadly in global land areas with large spatial variabilities (Figure 2b–k), and the magnitude of precipitation extreme changes is greater than that of mean precipitation. Under the SSP3-7.0 scenario, we found that the responses of precipitation extremes to land use change (ssp370-ssp126Lu-ssp370) also show large spatial variabilities, and the regions with robust changes in precipitation extremes are limited (Supplementary Materials Figure S6).

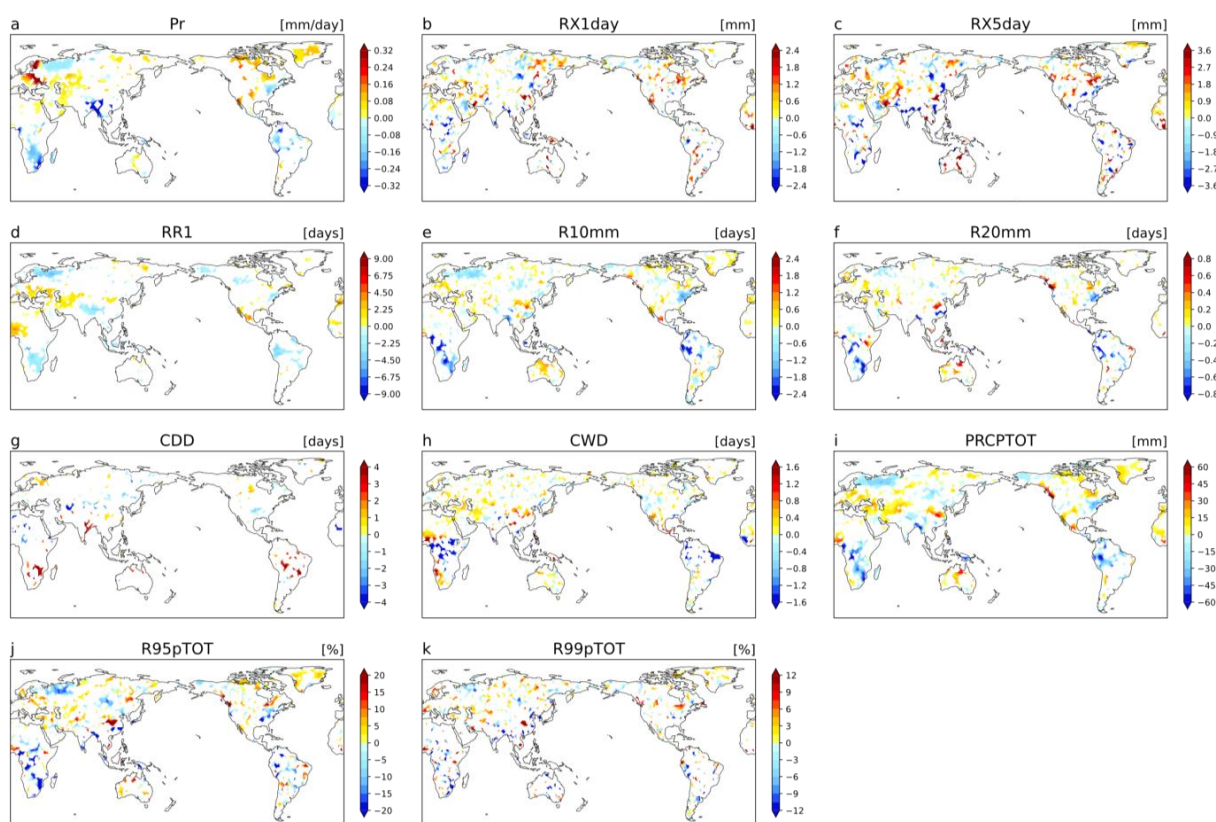


Figure 2. Similar to Figure 1 but for multi-model ensemble spatial patterns of the impact of land use change on future precipitation extremes. (a) mean precipitation, (b) RX1day, (c) RX5day, (d) RR1, (e) R10mm, (f) R20mm, (g) CDD, (h) CWD, (i) PRCPTOT, (j) R95pTOT, (k) R99pTOT.

3.2. Regional Contribution of Different Land Use Scenarios to Climate Extremes

To further examine the regional changes, in each of the 26 IPCC regions (Supplementary Materials Figure S4), we analyzed the relative contribution of land use change to future climate extremes compared with other anthropogenic forcings (Figure 3). The results show that under the SSP1-2.6 scenario, using the SSP3-7.0 land use scenario contributes most to temperature extreme changes over Central America/Mexico (ranging from -12.9% (TXn) to -4.5% (TNx)), Southern Europe/the Mediterranean (ranging from -14.0% (TNn) to -4.5% (TNx)), Central Europe (ranging from -8.5% (CSDI) to 10.3% (TXx)) and Western Asia (ranging from -2.8% (TN10p) to 7.2% (TXn)) (Figure 3a). Among the temperature extremes, the indices with the most significant relative contribution of the land use change (ssp126-370Lu–ssp126) across regions are TNx (ranging from -7.8% to 6.1%), TNn (ranging from -14.0% to 2.1%) and TXn (ranging from -11.5% to 7.2%). Under the SSP3-7.0 scenario, the contribution of using the SSP1-2.6 scenario to regional climate extremes is less significant, with the largest contribution to Western North America (ranging from -3.5% (TXn) to -0.3% (CSDI)) and Central America/Mexico (ranging from 3.0% (TX90p) to 4.7% (TXn)) (Supplementary Materials Figure S7a).

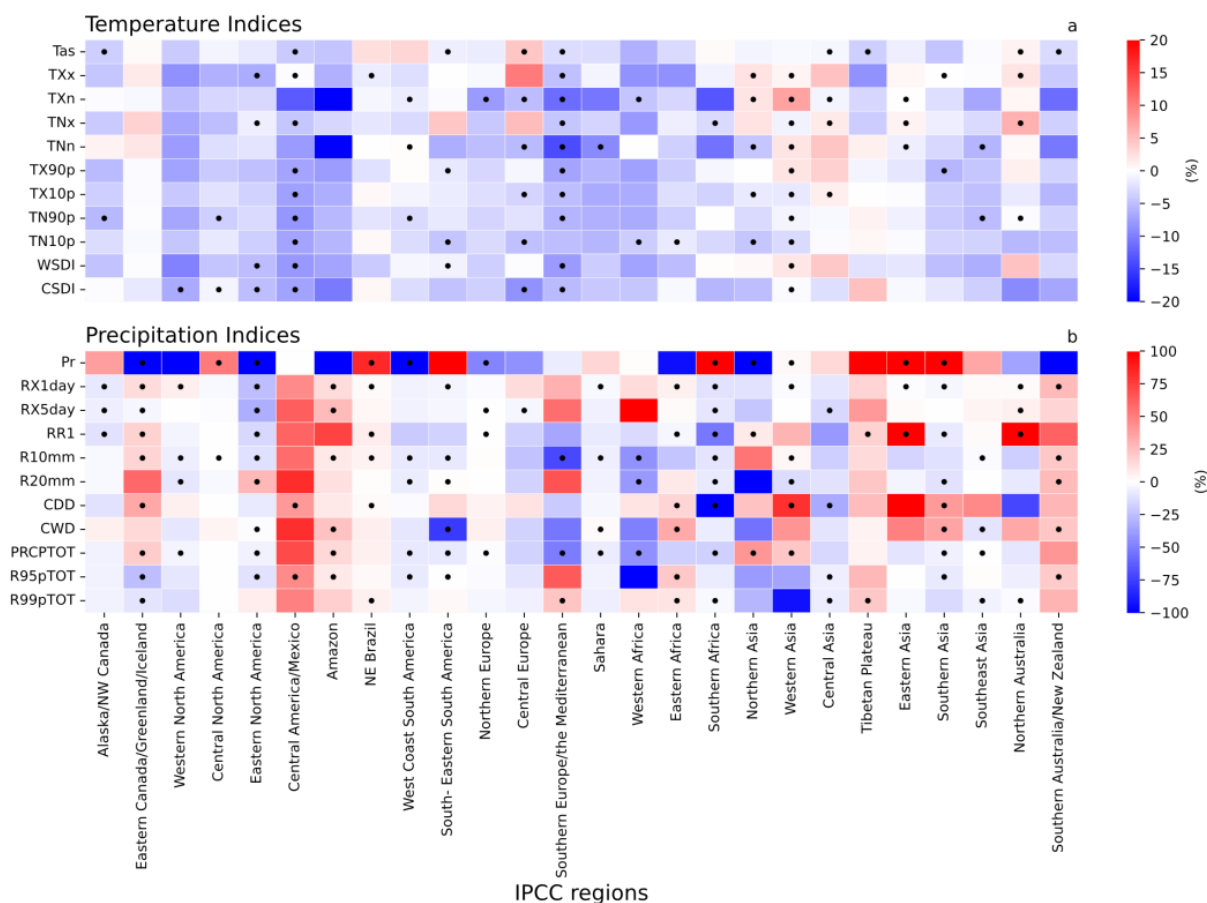


Figure 3. Under SSP1-2.6 scenario, the multi-model ensemble relative contribution of land use change (i.e., ssp126-ssp370lu–ssp126) to future changes in regional temperature extremes (a) and precipitation extremes (b); relative contributions are calculated relative to future regional projections with all other anthropogenic forcings for each of the extreme climate indices (see Methods). The 26 regions selected are defined by IPCC AR5 Reference Regions (Supplementary Materials Figure S4). A black dot is added when at least 80% of models simulate the same change sign in the region.

For regional precipitation extremes, the land use change has a relatively large contribution. Under the SSP1-2.6 scenario, use of the SSP3-7.0 land use scenario leads to the most significant changes over Eastern Canada/Greenland/Iceland (ranging

from -25.4% (R95pTOT) to 33.6% (CDD)), Eastern North America (ranging from -118.4% (Pr) to 27.8% (R20mm)), Southern Africa (ranging from -149.7% (CDD) to -2.8% (R99pTOT)) and Southern Asia (ranging from -11.3% (R20mm) to 39.2% (CWD)) (Figure 3b). The land use change (ssp126-370Lu-ssp126) contributes the most to changes in RX1day, RR1 and PRCPTOT, ranging from -52.9% to 138.8% . Under the SSP3-7.0 scenario, the contribution of land use change (ssp370-126Lu-ssp370) is significantly reduced (Supplementary Materials Figure S7b).

3.3. Global Contribution of Different Land Use Scenarios to Climate Extremes

Figure 4 shows the multi-model ensemble global-averaged relative contribution of land use change to climate extremes. Under the SSP1-2.6 scenario, the contribution of land use change (ssp126-370Lu-ssp126) to global mean temperature extremes is relatively small, ranging from -5.5% to -0.9% (Figure 4a), and it shows that the contribution to global-averaged temperature extremes is greater than that to mean temperature. Extreme indices with a significant contribution of land use change are TXn (-5.5%), TNn (-5.0%), TX90p (-2.7%), TX10p (-2.9%), TN10p (-3.3%), WSDI (-2.0%) and CSDI (-3.6%), of which at least 80% of the models simulate the same sign of global-averaged extreme change. Due to the large spread of ESMs' responses to LULCC, the contribution to TAS (from -6.4% (CMCC-ESM2) to 3.0% (CanESM5)), TXX (from -6.0% (CMCC-ESM2) to 4.2% (CNRM-ESM2-1)) and TNX (from -8.5% (BCC-CSM2-MR) to 7.2% (MPI-ESM1-2-LR)) spreads greatly between ESMs and is not statistically robust.

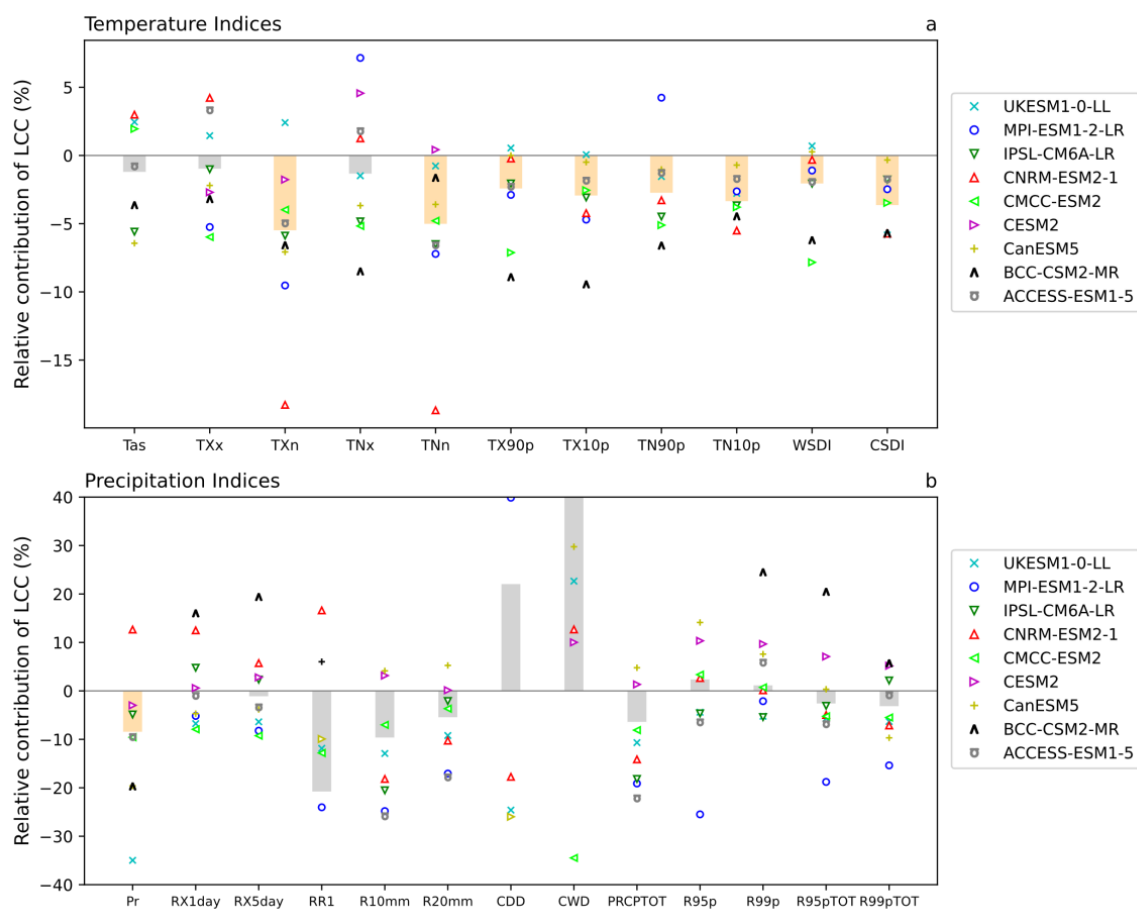


Figure 4. Under SSP1-2.6 scenario, the multi-model ensemble global-averaged relative contribution of land use change (i.e., ssp126-ssp370lu-ssp126) to temperature extremes (a) and precipitation extremes (b); relative contributions are calculated relative to future global projections with all other anthropogenic forcings (see Methods). Extreme climate indices are averaged over 2070–2099. Light yellow bars correspond to at least 80% of models simulating the same global change sign.

Figure 4b shows that the effects of land use change (ssp126-370Lu–ssp126) on precipitation extremes are much larger than those on temperature extremes, and the contribution to global mean precipitation extremes spreads largely, ranging from -20.8% to 103.0% . However, only the contribution of land use change to mean precipitation is robust, with a reduction in global mean precipitation by -8.4% . Furthermore, Figure 4b shows strong inter-model spreads of the contribution of land use change to precipitation extremes, with the largest contribution to CDD (from -70.9% (BCC-CSM2-MR) to 62.5% (ACCESS-ESM1-5)), CWD (from -127% (IPSL-CM6A-LR) to 121.9% (ACCESS-ESM1-5)) and R95pTOT (from 20.4% (BCC-CSM2-MR) to -18.8% (MPI-ESM1-2-LR)).

Under the SSP3-7.0 scenario, using the SSP1-2.6 land use scenario has little influence on global mean temperature extremes. The relative contribution of land use change (ssp370-126Lu–ssp370) to temperature extremes ranges from 0.2% to 1.3% (Supplementary Materials Figure S8a). Using the SSP1-2.6 land use scenario reduces the global mean temperature by -0.9% ; however, the signs of simulated change in ESMs are inconsistent for most temperature extremes. For precipitation, compared with the SSP1-2.6 scenario, the contribution of land use change to precipitation extreme changes is less, with a range from -6.7% to 22.3% . Using the SSP1-2.6 land use scenario reduces the global mean daily precipitation of more than 10 mm by -6.3% (Supplementary Materials Figure S8b). Due to the large spread among the model's responses, the contribution to most global-averaged precipitation extremes is not robust (Supplementary Materials Figure S8b).

4. Discussion and Conclusions

The future land use policy sensitivity experiments in LUMIP mainly focus on the impact of different land use scenarios on the climate; results from the experiments are against the assumption that a radiative forcing level can be achieved through various socioeconomic scenarios with a negligible effect on climate [43]. In other words, the ssp126 and ssp126-ssp370Lu simulations have the same radiative forcing level, but replacing SSP1-2.6 with the SSP3-7.0 land use scenario in the simulation has led to substantial changes in climate. Furthermore, the effects from LULCC are larger at regional scales in the simulations; thus, different spatial patterns of land use scenarios will change the projections of regional climate changes—for example, afforestation in middle and high latitudes with large albedo change would likely lead to larger climatic effects. This has implications for understanding the role of land use and land management in regional climate mitigation.

In contrast to the limitations of previous studies, which use single or a few models [10,11,16,17,19], more ESMs and a multi-model ensemble approach, as used in this study, can overcome the uncertainties of previous studies and obtain more robust results. Under the SSP1-2.6 scenario, the relative impact of LULCC (land use change between different land use scenarios) on temperature extremes is larger (can reach up to -14% for TNn) at the regional scale than that in previous analyses [10,24], which may be attributed to the various land use scenarios. Moreover, in contrast to previous studies [14,19,24], LULCC affects global climate extremes robustly for more extreme temperature indices (TXn, TNn, TX90p, TX10p, TN90p, TN10p, WSDI, CSDI) and less precipitation indices (only mean precipitation) in our results, which may be due to more ESMs being used in this study and the large spread of the model's response in precipitation. Under the SSP3-7.0 scenario, the relative effects of LULCC on climate extremes is smaller, mainly because radiative forcing in SSP3-7.0 is much larger than in SSP1-2.6.

LULCC affects temperature extremes mainly through two mechanisms: albedo-driven radiative forcing and evapotranspiration-driven nonradiative forcing (changes in latent and sensible heat fluxes). The albedo effect is predominant during winter and daytime, while the evapotranspiration effect dominates during summer and nighttime [19]. Our results show significant mid-latitude cooling of TXn (coldest day) and TNn (coldest night) as albedo increases with future land use change (Figure 1c,e), while TXx (warmest day) and TNx (warmest night) are warmed as evapotranspiration decreases with future land

use change (Figure 1b,d), which agrees well with earlier studies [5,14,24]. In addition, the tropical warming in mean temperature change to LULCC may increase warm days (TX90p) and warm nights (TX10p) and reduce cold days (TX10p) and cold nights (TN10p) in tropical regions, with similar findings for mid-latitude cooling in mean temperature and the changes in temperature duration extremes (TX90p, TX10p, TN90p, TN10p) in mid-latitudes (Figure 1a–i).

The response of precipitation extremes to LULCC shows large spatial variability, and mean precipitation change has little correlation with extreme precipitation change (Figure 2). The regional effects of LULCC on precipitation extremes are more robust and larger in magnitude than the global effects. In tropical regions with extensive deforestation in the land use scenario, deforestation leads to reduced transpiration and less water vapor available to form clouds, which in turn decreases the mean and extreme precipitation, consistent with previous studies [5,25].

The effects of LULCC on climate extremes differ strongly across models and regions in the simulations, especially for precipitation extremes, which is in line with previous analyses [11,13,23,44]. The model spread is affected by several factors. First, ESMs differ in the representation of LULCC due to various factors, including plant functional types, initial forest cover and vegetation dynamics. This leads to different spatial patterns of tree cover change among ESMs (Supplementary Materials Figures S1 and S2). Second, the parameterizations of the land surface process related to LULCC vary in ESMs. Third, there are large uncertainties associated with land–atmosphere interactions in ESMs. Therefore, more research on the observation-constrained model’s responses to LULCC is needed to reduce uncertainties in projections of climate extremes.

In summary, the results from ten Earth system models participating in the LUMIP future land use policy sensitivity experiment demonstrate that the use of different land use change scenarios has a substantial effect on the projections of regional climate extreme changes. Our study also reveals that, compared with other anthropogenic forcings, the land use change has a considerable contribution to regional temperature extreme changes, with the contribution ranging from -14.0% to 10.3% , and the contribution to regional precipitation extreme change is larger, with a range of -118.4% – 138.8% . The global climate effects of land use change are smaller in magnitude than regional effects, with a small (5%) contribution to temperature extremes. We find a large spread of the model’s response to land use change, suggesting that research on reducing models’ uncertainties is needed to obtain more robust future projections of regional extreme climate change. Our study highlights the essential role of land use and land management strategies in future regional climate mitigation.

Supplementary Materials: The following supporting information can be downloaded at: <https://www.mdpi.com/article/10.3390/atmos13060995/s1>, Figure S1: Time series of projected global average forest cover, cropland and pasture area under SSP1-2.6 and SSP3-7.0 land use scenarios (2015–2100); Figure S2: The differences of tree fraction cover changes (2100–2015) between ssp126-ssp370Lu and ssp126 simulation, performed by each CMIP6 model; Figure S3: Similar to Supplementary Figure S2 but for differences between ssp370-ssp126Lu and ssp370 simulation; Figure S4: Spatial boundaries of the geographical regions defined in the IPCC 5th Assessment Report; Figure S5: Similar to Figure 1 but for impact of land use change under SSP3-7.0 scenario (i.e. ssp370-ssp126lu-ssp370); Figure S6: Similar to Figure 2 but for impact of land use change under SSP3-7.0 scenario (i.e. ssp370-ssp126lu-ssp370); Figure S7: Similar to Figure 3 but for regional relative contribution of land use change (i.e. ssp370-ssp126lu-ssp370) under SSP3-7.0 scenario; Figure S8: Similar to Figure 4 but for global-averaged relative contribution of land use change (i.e. ssp370-ssp126lu-ssp370) under SSP3-7.0 scenario; Table S1: Definition and description of extreme temperature and extreme precipitation indices.

Author Contributions: Conceptualization, T.H. and J.W.; Methodology, T.H.; Validation, M.Y.; Visualization, X.K.; Writing—original draft, T.H.; Writing—review and editing, J.W., X.K., M.Y. and L.D. All authors have read and agreed to the published version of the manuscript.

Funding: This research was funded by the Independent Research Project of Key Laboratory of Flight Techniques and Flight Safety, CAAC (FZ2020ZZ03).

Institutional Review Board Statement: Not applicable.

Informed Consent Statement: Not applicable.

Data Availability Statement: The data that support the reported results are available from the first author upon request.

Acknowledgments: We (T.H., J.W., X.K., M.Y. and L.D.) thank the three anonymous reviewers and editors for their invaluable comments and suggestions on this paper.

Conflicts of Interest: The authors declare no conflict of interest.

References

1. Mahmood, R.; Pielke, R.A.; Hubbard, K.G.; Niyogi, D.; Dirmeyer, P.A.; McAlpine, C.; Carleton, A.M.; Hale, R.; Gameda, S.; Beltrán-Przekurat, A.; et al. Land Cover Changes and Their Biogeophysical Effects on Climate: Land cover changes and their biogeophysical effects on climate. *Int. J. Climatol.* **2014**, *34*, 929–953. [[CrossRef](#)]
2. Pielke, R.A.; Pitman, A.; Niyogi, D.; Mahmood, R.; McAlpine, C.; Hossain, F.; Goldewijk, K.K.; Nair, U.; Betts, R.; Fall, S.; et al. Land Use/Land Cover Changes and Climate: Modeling Analysis and Observational Evidence. *WIREs Clim. Chang.* **2011**, *2*, 828–850. [[CrossRef](#)]
3. Quesada, B.; Arneth, A.; Robertson, E.; de Noblet-Ducoudré, N. Potential Strong Contribution of Future Anthropogenic Land-Use and Land-Cover Change to the Terrestrial Carbon Cycle. *Environ. Res. Lett.* **2018**, *13*, 064023. [[CrossRef](#)]
4. Lejeune, Q.; Seneviratne, S.I.; Davin, E.L. Historical Land-Cover Change Impacts on Climate: Comparative Assessment of LUCID and CMIP5 Multimodel Experiments. *J. Clim.* **2017**, *30*, 1439–1459. [[CrossRef](#)]
5. Quesada, B.; Arneth, A.; de Noblet-Ducoudré, N. Atmospheric, Radiative, and Hydrologic Effects of Future Land Use and Land Cover Changes: A Global and Multimodel Climate Picture: Climatic Effects of Future LULCC. *J. Geophys. Res. Atmos.* **2017**, *122*, 5113–5131. [[CrossRef](#)]
6. Boisier, J.P.; de Noblet-Ducoudré, N.; Pitman, A.J.; Cruz, F.T.; Delire, C.; van den Hurk, B.J.J.M.; van der Molen, M.K.; Müller, C.; Voldoire, A. Attributing the Impacts of Land-Cover Changes in Temperate Regions on Surface Temperature and Heat Fluxes to Specific Causes: Results from the First LUCID Set of Simulations: Biogeophysical Impacts of Lulcc. *J. Geophys. Res.* **2012**, *117*, D12116. [[CrossRef](#)]
7. Lee, X.; Goulden, M.L.; Hollinger, D.Y.; Barr, A.; Black, T.A.; Bohrer, G.; Bracho, R.; Drake, B.; Goldstein, A.; Gu, L.; et al. Observed Increase in Local Cooling Effect of Deforestation at Higher Latitudes. *Nature* **2011**, *479*, 384–387. [[CrossRef](#)]
8. Li, Y.; Zhao, M.; Motesharrei, S.; Mu, Q.; Kalnay, E.; Li, S. Local Cooling and Warming Effects of Forests Based on Satellite Observations. *Nat. Commun* **2015**, *6*, 6603. [[CrossRef](#)]
9. De Noblet-Ducoudré, N.; Boisier, J.-P.; Pitman, A.; Bonan, G.B.; Brovkin, V.; Cruz, F.; Delire, C.; Gayler, V.; van den Hurk, B.J.J.M.; Lawrence, P.J.; et al. Determining Robust Impacts of Land-Use-Induced Land Cover Changes on Surface Climate over North America and Eurasia: Results from the First Set of LUCID Experiments. *J. Clim.* **2012**, *25*, 3261–3281. [[CrossRef](#)]
10. Chen, L.; Dirmeyer, P.A. The Relative Importance among Anthropogenic Forcings of Land Use/Land Cover Change in Affecting Temperature Extremes. *Clim. Dyn.* **2019**, *52*, 2269–2285. [[CrossRef](#)]
11. Boysen, L.R.; Brovkin, V.; Arora, V.K.; Cadule, P.; de Noblet-Ducoudré, N.; Kato, E.; Pongratz, J.; Gayler, V. Global and Regional Effects of Land-Use Change on Climate in 21st Century Simulations with Interactive Carbon Cycle. *Earth Syst. Dyn.* **2014**, *5*, 309–319. [[CrossRef](#)]
12. Davies-Barnard, T.; Valdes, P.J.; Singarayer, J.S.; Pacifico, F.M.; Jones, C.D. Full Effects of Land Use Change in the Representative Concentration Pathways. *Environ. Res. Lett.* **2014**, *9*, 114014. [[CrossRef](#)]
13. Brovkin, V.; Boysen, L.; Arora, V.K.; Boisier, J.P.; Cadule, P.; Chini, L.; Claussen, M.; Friedlingstein, P.; Gayler, V.; van den Hurk, B.J.J.M.; et al. Effect of Anthropogenic Land-Use and Land-Cover Changes on Climate and Land Carbon Storage in CMIP5 Projections for the Twenty-First Century. *J. Clim.* **2013**, *26*, 6859–6881. [[CrossRef](#)]
14. Pitman, A.J.; de Noblet-Ducoudré, N.; Avila, F.B.; Alexander, L.V.; Boisier, J.-P.; Brovkin, V.; Delire, C.; Cruz, F.; Donat, M.G.; Gayler, V.; et al. Effects of Land Cover Change on Temperature and Rainfall Extremes in Multi-Model Ensemble Simulations. *Earth Syst. Dyn.* **2012**, *3*, 213–231. [[CrossRef](#)]
15. Lejeune, Q.; Davin, E.L.; Gudmundsson, L.; Winckler, J.; Seneviratne, S.I. Historical Deforestation Locally Increased the Intensity of Hot Days in Northern Mid-Latitudes. *Nat. Clim. Chang.* **2018**, *8*, 386–390. [[CrossRef](#)]
16. Avila, F.B.; Pitman, A.J.; Donat, M.G.; Alexander, L.V.; Abramowitz, G. Climate Model Simulated Changes in Temperature Extremes due to Land Cover Change: Changes in Climate Extremes due to Lulcc. *J. Geophys. Res.* **2012**, *117*, D04108. [[CrossRef](#)]
17. Findell, K.L.; Berg, A.; Gentine, P.; Krasting, J.P.; Lintner, B.R.; Malyshev, S.; Santanello, J.A.; Shevliakova, E. The Impact of Anthropogenic Land Use and Land Cover Change on Regional Climate Extremes. *Nat. Commun.* **2017**, *8*, 989. [[CrossRef](#)] [[PubMed](#)]

18. Li, X.; Chen, H.; Wei, J.; Hua, W.; Sun, S.; Ma, H.; Li, X.; Li, J. Inconsistent Responses of Hot Extremes to Historical Land Use and Cover Change among the Selected CMIP5 Models. *J. Geophys. Res. Atmos.* **2018**, *123*, 3497–3512. [[CrossRef](#)]
19. Christidis, N.; Stott, P.A.; Hegerl, G.C.; Betts, R.A. The Role of Land Use Change in the Recent Warming of Daily Extreme Temperatures: Land Use Change and Temperature Extremes. *Geophys. Res. Lett.* **2013**, *40*, 589–594. [[CrossRef](#)]
20. Mueller, N.D.; Butler, E.E.; McKinnon, K.A.; Rhines, A.; Tingley, M.; Holbrook, N.M.; Huybers, P. Cooling of US Midwest Summer Temperature Extremes from Cropland Intensification. *Nat. Clim. Chang.* **2016**, *6*, 317–322. [[CrossRef](#)]
21. Thiery, W.; Visser, A.J.; Fischer, E.M.; Hauser, M.; Hirsch, A.L.; Lawrence, D.M.; Lejeune, Q.; Davin, E.L.; Seneviratne, S.I. Warming of Hot Extremes Alleviated by Expanding Irrigation. *Nat. Commun.* **2020**, *11*, 290. [[CrossRef](#)] [[PubMed](#)]
22. Niu, X.; Tang, J.; Wang, S.; Fu, C. Impact of Future Land Use and Land Cover Change on Temperature Projections over East Asia. *Clim Dyn.* **2019**, *52*, 6475–6490. [[CrossRef](#)]
23. Hirsch, A.L.; Guillod, B.P.; Seneviratne, S.I.; Beyerle, U.; Boysen, L.R.; Brovkin, V.; Davin, E.L.; Doelman, J.C.; Kim, H.; Mitchell, D.M.; et al. Biogeophysical Impacts of Land-Use Change on Climate Extremes in Low-Emission Scenarios: Results from HAPPI-Land. *Earth's Future* **2018**, *6*, 396–409. [[CrossRef](#)] [[PubMed](#)]
24. Sy, S.; Quesada, B. Anthropogenic Land Cover Change Impact on Climate Extremes during the 21st Century. *Environ. Res. Lett.* **2020**, *15*, 034002. [[CrossRef](#)]
25. Perugini, L.; Caporaso, L.; Marconi, S.; Cescatti, A.; Quesada, B.; de Noblet-Ducoudré, N.; House, J.I.; Arneth, A. Biophysical Effects on Temperature and Precipitation due to Land Cover Change. *Environ. Res. Lett.* **2017**, *12*, 053002. [[CrossRef](#)]
26. Hirsch, A.L.; Wilhelm, M.; Davin, E.L.; Thiery, W.; Seneviratne, S.I. Can Climate-effective Land Management Reduce Regional Warming? *J. Geophys. Res. Atmos.* **2017**, *122*, 2269–2288. [[CrossRef](#)]
27. Boysen, L.R.; Brovkin, V.; Pongratz, J.; Lawrence, D.M.; Lawrence, P.; Vuichard, N.; Peylin, P.; Liddicoat, S.; Hajima, T.; Zhang, Y.; et al. Global Climate Response to Idealized Deforestation in CMIP6 Models. *Biogeosciences* **2020**, *17*, 5615–5638. [[CrossRef](#)]
28. Cherubini, F.; Huang, B.; Hu, X.; Tölle, M.H.; Strømman, A.H. Quantifying the Climate Response to Extreme Land Cover Changes in Europe with a Regional Model. *Environ. Res. Lett.* **2018**, *13*, 074002. [[CrossRef](#)]
29. Hu, X.; Huang, B.; Cherubini, F. Impacts of Idealized Land Cover Changes on Climate Extremes in Europe. *Ecol. Indic.* **2019**, *104*, 626–635. [[CrossRef](#)]
30. Popp, A.; Calvin, K.; Fujimori, S.; Havlik, P.; Humpenöder, F.; Stehfest, E.; Bodirsky, B.L.; Dietrich, J.P.; Doelmann, J.C.; Gusti, M.; et al. Land-Use Futures in the Shared Socio-Economic Pathways. *Glob. Environ. Chang.* **2017**, *42*, 331–345. [[CrossRef](#)]
31. Lawrence, D.M.; Hurtt, G.C.; Arneth, A.; Brovkin, V.; Calvin, K.V.; Jones, A.D.; Jones, C.D.; Lawrence, P.J.; de Noblet-Ducoudré, N.; Pongratz, J.; et al. The Land Use Model Intercomparison Project (LUMIP) Contribution to CMIP6: Rationale and Experimental Design. *Geosci. Model Dev.* **2016**, *9*, 2973–2998. [[CrossRef](#)]
32. Eyring, V.; Bony, S.; Meehl, G.A.; Senior, C.A.; Stevens, B.; Stouffer, R.J.; Taylor, K.E. Overview of the Coupled Model Intercomparison Project Phase 6 (CMIP6) Experimental Design and Organization. *Geosci. Model Dev.* **2016**, *9*, 1937–1958. [[CrossRef](#)]
33. Ziehn, T.; Chamberlain, M.A.; Law, R.M.; Lenton, A.; Bodman, R.W.; Dix, M.; Stevens, L.; Wang, Y.-P.; Srbiniovsky, J. The Australian Earth System Model: ACCESS-ESM1.5. *J. South. Hemisph. Earth Syst. Sci.* **2020**, *70*, 193. [[CrossRef](#)]
34. Wu, T.; Lu, Y.; Fang, Y.; Xin, X.; Li, L.; Li, W.; Jie, W.; Zhang, J.; Liu, Y.; Zhang, L.; et al. The Beijing Climate Center Climate System Model (BCC-CSM): The Main Progress from CMIP5 to CMIP6. *Geosci. Model Dev.* **2019**, *12*, 1573–1600. [[CrossRef](#)]
35. Swart, N.C.; Cole, J.N.S.; Kharin, V.V.; Lazare, M.; Scinocca, J.F.; Gillett, N.P.; Anstey, J.; Arora, V.; Christian, J.R.; Hanna, S.; et al. The Canadian Earth System Model Version 5 (CanESM5.0.3). *Geosci. Model Dev.* **2019**, *12*, 4823–4873. [[CrossRef](#)]
36. Danabasoglu, G.; Lamarque, J.-F.; Bacmeister, J.; Bailey, D.A.; DuVivier, A.K.; Edwards, J.; Emmons, L.K.; Fasullo, J.; Garcia, R.; Gettelman, A.; et al. The Community Earth System Model Version 2 (CESM2). *J. Adv. Model. Earth Syst.* **2020**, *12*, e2019MS001916. [[CrossRef](#)]
37. Cherchi, A.; Fogli, P.G.; Lovato, T.; Peano, D.; Iovino, D.; Gualdi, S.; Masina, S.; Scoccimarro, E.; Materia, S.; Bellucci, A.; et al. Global Mean Climate and Main Patterns of Variability in the CMCC-CM2 Coupled Model. *J. Adv. Model. Earth Syst.* **2019**, *11*, 185–209. [[CrossRef](#)]
38. Séférian, R.; Nabat, P.; Michou, M.; Saint-Martin, D.; Voldoire, A.; Colin, J.; Decharme, B.; Delire, C.; Berthet, S.; Chevallier, M.; et al. Evaluation of CNRM Earth System Model, CNRM-ESM2-1: Role of Earth System Processes in Present-Day and Future Climate. *J. Adv. Model. Earth Syst.* **2019**, *11*, 4182–4227. [[CrossRef](#)]
39. Boucher, O.; Servonnat, J.; Albright, A.L.; Aumont, O.; Balkanski, Y.; Bastrikov, V.; Bekki, S.; Bonnet, R.; Bony, S.; Bopp, L.; et al. Presentation and Evaluation of the IPSL-CM6A-LR Climate Model. *J. Adv. Model. Earth Syst.* **2020**, *12*, e2019MS002010. [[CrossRef](#)]
40. Mauritsen, T.; Bader, J.; Becker, T.; Behrens, J.; Bittner, M.; Brokopf, R.; Brovkin, V.; Claussen, M.; Crueger, T.; Esch, M.; et al. Developments in the MPI-M Earth System Model Version 1.2 (MPI-ESM1.2) and Its Response to Increasing CO₂. *J. Adv. Model. Earth Syst.* **2019**, *11*, 998–1038. [[CrossRef](#)]
41. Seland, Ø.; Bentsen, M.; Seland Graff, L.; Olivié, D.; Toniazzo, T.; Gjermundsen, A.; Debernard, J.B.; Gupta, A.K.; He, Y.; Kirkevåg, A.; et al. The Norwegian Earth System Model, NorESM2—Evaluation of TheCMIP6 DECK and Historical Simulations. *Clim. Earth Syst. Model.* **2020**. preprint. [[CrossRef](#)]
42. Sellar, A.A.; Jones, C.G.; Mulcahy, J.P.; Tang, Y.; Yool, A.; Wiltshire, A.; O'Connor, F.M.; Stringer, M.; Hill, R.; Palmieri, J.; et al. UKESM1: Description and Evaluation of the U.K. Earth System Model. *J. Adv. Model. Earth Syst.* **2019**, *11*, 4513–4558. [[CrossRef](#)]

43. van Vuuren, D.P.; Kriegler, E.; O'Neill, B.C.; Ebi, K.L.; Riahi, K.; Carter, T.R.; Edmonds, J.; Hallegatte, S.; Kram, T.; Mathur, R.; et al. A New Scenario Framework for Climate Change Research: Scenario Matrix Architecture. *Clim. Chang.* **2014**, *122*, 373–386. [[CrossRef](#)]
44. Pitman, A.J.; de Noblet-Ducoudré, N.; Cruz, F.T.; Davin, E.L.; Bonan, G.B.; Brovkin, V.; Claussen, M.; Delire, C.; Ganzeveld, L.; Gayler, V.; et al. Uncertainties in Climate Responses to Past Land Cover Change: First Results from the LUCID Intercomparison Study. *Geophys. Res. Lett.* **2009**, *36*, L14814. [[CrossRef](#)]